fuels

MDPI

Article

Performance of Citric Acid as a Catalyst and Support Catalyst When Synthesized with NaOH and CaO in Transesterification of Biodiesel from Black Soldier Fly Larvae Fed on Kitchen Waste

Lilies K. Kathumbi [1,*], Patrick G. Home [2], James M. Raude [2] and Benson B. Gathitu [3]

[1] Institute for Basic Sciences, Technology and Innovation, Department of Civil Engineering, Pan African University, Nairobi P.O. Box 62000-00200, Kenya
[2] Department of Soil, Water and Environmental Engineering, Jomo Kenyatta University of Agriculture and Technology, Nairobi P.O. Box 62000-00200, Kenya; pghome@jkuat.ac.ke (P.G.H.); ramesso@jkuat.ac.ke (J.M.R.)
[3] Department of Agricultural and Biosystems Engineering, Jomo Kenyatta University of Agriculture and Technology, Nairobi P.O. Box 62000-00200, Kenya; bbgathitu@jkuat.ac.ke
* Correspondence: lilieskath@gmail.com; Tel.: +254-722813031

Abstract: Current research and development to lower the production cost of biodiesel by utilizing feedstock derived from waste motivates the quest for developing catalysts with high performance in transesterification. This study investigates the performance of citric acid as a catalyst and support catalyst in transesterification of oil from black soldier fly (*Hermetia illucens*) larvae fed on organic kitchen waste. Two catalysts were prepared by synthesizing citric acid with NaOH and CaO by a co-precipitation and an impregnation method, respectively. The design of the experiment adopted response surface methodology for the optimization of biodiesel productivity by varying: the percentage loading weight of citric acid, the impregnation temperature, the calcinating temperature and the calcinating time. The characteristic activity and reuse of the synthesized catalysts in transesterification reactions were investigated. The morphology, chemical composition and structure of the catalysts were characterized by scanning electron microscopy (SEM), Fourier transform infrared (FTIR) spectroscopy, X-ray fluorescence (XRF) and X-ray diffraction (XRD). High citric acid loading on NaOH and a small amount of citric acid on CaO resulted in improved dispersion and refinement of the particle sizes. Increasing citric acid loading on NaOH improved the CaO and SiO_2 composition of the modified catalyst resulting in higher biodiesel yield compared to the modified CaO catalyst. A maximum biodiesel yield of 93.08%, ±1.31, was obtained when NaOH was synthesized with a 130% weight of citric acid at 80 °C and calcinated at 600 °C for 240 min. Comparatively, a maximum biodiesel yield of 90.35%, ±1.99, was obtained when CaO was synthesized with a 3% weight of citric acid, impregnated at 140 °C and calcinated at 900 °C for 240 min. The two modified catalysts could be recycled four times while maintaining a biodiesel yield of more than 70%.

Keywords: black soldier fly; biodiesel conversion; catalyst characterization; synthesis catalyst; transesterification process; kitchen waste

Citation: Kathumbi, L.K.; Home, P.G.; Raude, J.M.; Gathitu, B.B. Performance of Citric Acid as a Catalyst and Support Catalyst When Synthesized with NaOH and CaO in Transesterification of Biodiesel from Black Soldier Fly Larvae Fed on Kitchen Waste. *Fuels* **2022**, *3*, 295–315. https://doi.org/10.3390/fuels3020018

Academic Editor: Maria A. Goula

Received: 28 March 2022
Accepted: 25 April 2022
Published: 17 May 2022

1. Introduction

Biodiesel is a promising alternative for fossil fuels with added environmental benefits. However, challenges to achieve sustainable and cost-effective production make decarbonization of the transport sector difficult [1]. Current research is directed toward realizing cost-effective feedstock and a production process with fewer production steps, a shorter production period and low energy input. Use of waste resources such as: waste cooking oil [2], municipal sludge [3], wastewater-based microalgae [4], food waste [5] and organic waste bioconversion using Black Soldier Fly Larvae (BSFL) [6,7] is gaining research attraction for third-generation biofuel production to mitigate food-versus-fuel competition. Third-generation biofuels are produced from organic waste and products. Hence, they are

linked to biological carbon fixation and carbon negative benefits to the environment [8]. Regardless of cost-competitive feedstock from non-edible oil sources, biodiesel production is faced with difficulty mainly attributed to the high free fatty acids (FFA) percentage and water content in the oil from waste resources that necessitates an intensive pre-treatment process [9].

Technologies available for producing biodiesel have been reported by Aransiola et al. [9] and Baskar and Aiswarya [10]. Among these technologies, catalytic transesterification is the most economic for industrial-level biodiesel production [11]. Catalysts used in the transesterification of triglycerides are classified as homogenous acid or base, heterogenous acid, base or solid catalysts, lipase/enzymes [12], transitional metals and silicate catalysts [13]. The selection of the type of catalyst highly depends on the percentage of FFA present in the oil. While homogenous catalysts are inexpensive and have high reaction rates, their operation is inhibited by the high percentage of FFA content in oils and the high water content in oil which leads to the formation of soap and difficulty in separating it from the biodiesel, making product recovery tedious [14,15].

Heterogenous catalysts are becoming more attractive for transesterification due to their ease of recovery, reusability, tolerance to moisture and high FFA content of the oil [15,16]. Overall, heterogenous catalysts have been reported to lower biodiesel production costs by 4–20%, hence attracting current studies to develop catalysts with high stability and anticipated chemical and physical properties [17]. Current research in transesterification is being directed to the development of environmentally friendly heterogenous alkali- or acid-based catalysts [18–22].

Synthesizing two or more compounds to produce a catalyst with increased catalyst active sites, acidity and basicity is a common phenomenon that is used to develop heterogenous catalysts with high reactivity, reusability and ease of separation [22,23]. The synthesis method used in catalyst development plays a major role in enhancing the catalytic properties. Catalyst synthesis routes are still under development. Some of the efficient methods that have been reported include impregnation methods [24], a hydrothermal method [25], co-precipitation [26], sol-gel [27], complexation [28] and freeze/spray drying [29]. Among these methods, coprecipitation and impregnation are becoming attractive as they require lower temperatures and yield high-purity crystalline powders [26].

The synthesis method and the calcination temperatures have been reported as the major parameters that influence textural properties, size, BrØnsted/Lewis acid sites and strength of catalysts [23,30]. Researchers have reported different optimal calcination temperatures for the synthesis of various catalysts: 400 °C for CaO/TiO_2-ZrO_2 [23], 600 °C for MoO_3/AL_2O_3 with citric acid (CA) [24], 500 °C for HZSM-5 with CA [22], 800 °C for NaCl/oyster shell [18] and 600 °C for KF/CaO [31].

For economical biodiesel production, the development of catalysts at lower reaction temperatures of less than 150 °C, low operation pressure and with a focus on solid acid catalysts need further research [32]. CA is currently gaining popularity as a green catalyst due to its role as a dealuminating, reducing and/or chelating agent when synthesized with metal oxides and rare-earth metals such as zinc–aluminium mixed oxides, zeolites HZSM-5, $LaMnO_3$ and MoO_3/AL_2O_3 [22,24,28,32,33]. CA is a tricarboxylic acid that bears three carboxyl groups and a hydroxyl group that can be deprotonated, making it possible to chemically react with metal hydroxides such as NaOH and $Ca(OH)_2$ by an ionic bond and weak covalence [34–36].

Synthesizing catalysts with citric acid has been reported to increase the surface dispersion of the catalyst, hence improving catalytic activity and yield in methanation as well as hydrocarbon oxidation [24,37]. Calcinating limestone with CA at 700 °C results in highly porous CaO with improved catalytic activity [38]. CA has been investigated as a catalyst in methane production as well as in the food and pharmaceutical industries. However, research on citric acid as a catalyst in biodiesel production still remains rare. Vieira et al. [22] investigated the effect of modifying MHSZ-5 with CA by varying the CA

concentration and treatment temperature on biodiesel yield and reported that the synthesis increases the acidity strength and the external surface area of the catalyst.

A study by Macina et al. [39] reported the possibility of synthesizing CA with sodium hydroxide through a hydrothermal synthesis process to form a carbon-dot catalyst with a high biodiesel yield. Sodium citrate is insoluble in methanol, making it a feasible heterogenous catalyst for biodiesel production. A cost-efficient and environmentally friendly method for the synthesis of sodium hydroxide with CA by coprecipitation to form anhydrous trisodium citric has also been reported by [40]. This method was invented for application in food processing and in the pharmaceutical industries but has not been investigated for biodiesel production. Previous studies have reported the effects of synthesizing a catalyst with CA, but it is unclear for the effects of the amount of CA on the modified catalyst and the biodiesel yield.

In this study, a homogenous catalyst (NaOH) and an heterogenous catalyst (CaO) are synthesized with citric acid by co-precipitation and impregnation, respectively, to determine their performance in the transesterification of BSFL oil. The design of the experiment adopted the response surface method (RSM) based on a four factor three-level, central composite design (CCD) to optimize biodiesel yield by varying the synthesis temperature, the CA% loading weight (CA wt.%), the calcination temperature and the time. For comparison purposes, biodiesel was also produced by the CaO as well as by citric acid alone before the synthesis.

2. Materials and Methods

2.1. Black Soldier Fly Larvae (BSFL) Rearing

BSFL were reared on kitchen waste at Jomo Kenyatta University of Agriculture and Technology, Kenya. BSFL was chosen as the feedstock for biodiesel production in this research due to its ability to convert biowaste into sustainable products and its ability to survive in tropical regions. After hatching, larvae were fed on starter feed for 5 days and thereafter fed on organic kitchen waste food for 28 days when they separated themselves from the food waste. BSFL were harvested after 33 days, washed and rinsed in deionized water. The clean BSFL were deactivated in an oven at 115 °C for 10 min, dried at 85 °C for overnight and thereafter ground using a domestic kitchen blender [41]. The BSFL biomass was then stored in a dry container ready for oil extraction.

2.2. Oil Extraction

A solvent extraction method was applied to extract lipids from the BSFL biomass using the Bligh and Dyer method [42]. Specifically, n-hexane was used at a solvent to biomass volume ratio of 3:1. The solvent was added to a volumetric flask with the BSFL biomass, mixed using a shaker at 150 rpm for 20 min and left in situ overnight. The liquid layer containing solvent and lipids was then collected by decantation and separated on a separatory funnel overnight. Oil was recovered from the solvent using a rotary evaporator. The extracted oil was washed using deionized water, dried in the oven at 100 °C and stored at 4 °C.

2.3. Preparation of the Catalysts

CaO samples were synthesised with CA by an impregnation method following the procedure reported by Kandaramath et al. [43]. Specifically, 2 g of CaO (AR grade, 98%) was added to a solution of CA (weight %) and glycine in 50 mL of deionized water. This was then mixed until a solution was attained and kept for 2 h under continuous stirring at room temperature. The solution was then dried at 100 °C to form a solid. For NaOH, synthesis with CA was performed by co-precipitation [40]. Specifically, 2 g of NaOH (AR grade, 98%) were diluted in 10 mL of deionized water with 1 g of glycine as a surfactant under stirring. CA was added, and the homogenous solution was heated to 40 °C, then cooled to room temperature to allow precipitation. The solution was centrifuged at 75 rpm to collect the precipitate, then dried at 130 °C. Thereafter, the synthesized catalysts were

calcinated in a furnace at 500–900 °C for 4 h. The effects of the CA weight %, the synthesis temperature, the calcination temperature and the period on the precursors were evaluated on percentage biodiesel yield.

For each base catalyst, three samples corresponding to different CA weight % were obtained. The samples were denoted as NaOH/3%CA, NaOH/66.5%CA and NaOH/130%CA, for NaOH-modified catalysts, and CaO/3%CA, CaO/66.5%CA and CaO/130%CA, for CaO-modified catalysts, respectively. CA and CaO as catalysts were also evaluated based on biodiesel yield.

2.4. Characterization of the Catalysts

The functional groups of the modified catalysts were analysed at room temperature on a Bruker Alpha Fourier FTIR spectrometer equipped with a deuterated triglycine sulfate detector and a temperature-controlled diamond attenuated total reflectance (ATR) accessory. All spectra were obtained at a range of 4000–400 cm^{-1} and a resolution of 4 cm^{-1}. The chemical composition of the samples was determined by XRF analysis using a Philips PW4024 Spectrometer. The basicity of the solid surfaces was determined by a titration method using benzene and benzoic acid with bromothymol blue as indicators [44]. The morphology and average sizes of the prepared heterogenous catalysts were observed and characterized by SEM (JEOL JCM 7000). The samples were glued to the stud and examined at 20 µm and 1200× magnification. The structural and crystalline properties were characterized by X-ray diffraction on a Rigaku Miniflex benchtop XRD using Cu Kα radiation (40 kV, 40 Ma, $\lambda = 1.5426$ Å). Diffractograms were obtained from 20° to 80° at 2θ at a step seize of 0.02. The average microcrystalline size (D) of the catalyst was calculated using Scherrer's Equation (1) [45].

$$D = K\frac{\lambda}{\beta\, cos\theta} \tag{1}$$

where D = crystalline size (nm), K = constant in respect to crystalline shape factor (0.89), λ = X-ray beam wavelength ($\lambda = 0.1542$ nm), β = full width at half-maximum intensity and θ = Bragg diffraction angle.

2.5. Experimental Design and Statistical Analysis

The effect of the CA wt.%, the synthesis temperature, the calcination temperature and the time on biodiesel yield was evaluated. RSM was adopted to provide insights on catalyst preparation factors for optimal biodiesel yield [45]. The model was adopted due to its ability to provide insightful data on testing, goodness of fit and graphical presentation of variables against the biodiesel yield. The response which is the biodiesel yield (%) was calculated using Equation (2).

$$Biodiesel\ yield(\%) = \frac{biodiesel\ produced\ (g)}{amount\ of\ oil\ used\ (g)} \times 100 \tag{2}$$

Design expert 11 was used for regression analysis and analysis of variance (ANOVA). The functional Equation (3) was applied to determine coefficients and correlation of central composite design (CCD) dependent and independent variables. Experiments were performed to confirm the predicted yield.

$$\begin{aligned} Y = \ & \beta_0 + \beta_1 X_1 + \beta_2 X_2 + \beta_3 X_3 + \beta_4 X_4 + \beta_{11} {X_1}^2 + \beta_{22} {X_2}^2 + \beta_{33} {X_3}^2 + \beta_{44} {X_4}^2 \\ & + \beta_{12} X_1 X_2 + \beta_{13} X_1 X_3 + \beta_{14} X_1 X_4 + \beta_{23} X_2 X_3 + \beta_{24} X_2 X_4 \\ & + \beta_{34} X_3 X_4 \end{aligned} \tag{3}$$

where Y = predicted biodiesel yield (%); X_1 = CA loading (CA wt.%); X_2 = synthesis temperature; X_3 = calcination temperature; X_4 = calcination time, β_0 = regression coefficient for the intercept, $\beta_1 - \beta_4$ are linear parameters, β_{12}, β_{13}, β_{14}, β_{23}, β_{24} and β_{34} = interaction parameters and β_{11}, β_{22}, β_{33} and β_{44} are quadratic parameters.

2.6. Transesterification Reaction

Transesterification is the reaction between triglycerides and alcohol in the presence of catalysts to form methyl/ethyl esters and glycerol as a by-product [46–48]. In this study, a two-step esterification of BSFL oil in 1% H_2SO_4 in methanol followed by transesterification using the synthesized catalysts in methanol was adopted. For the transesterification reaction, 4 g of oil, 2.5 wt.% of catalyst, and an oil–methanol ratio of 1:8 was reacted in a 250 mL conical flask on a temperature-controlled hot plate equipped with a magnetic stirrer. The mixture was heated at 75 °C with stirring for 40 min. After cooling, a centrifuge was used to aid the separation of methanol, methyl esters, glycerol and the catalyst. A separating funnel was used to collect the upper layer containing biodiesel and methanol. A rotary evaporator was then used to recover methanol from the biodiesel. The biodiesel was then washed with warm deionized water, dried and weighed to determine the percentage yield. An equation of the transesterification reaction is presented in Figure 1 [49].

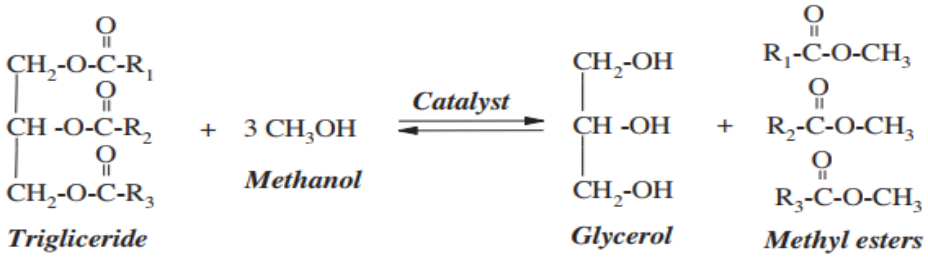

Figure 1. Transesterification reaction, where R_1, R_2, and R_3 are long hydrocarbon bonds.

The reaction is reversible, hence the need for excess alcohol to shift the equilibrium toward the formation of ethyl/methyl esters [50].

2.7. Biodiesel Characterization

The biodiesel functional groups were characterized by a Bruker Alpha FTIR spectrometer as reported in Section 2.4. The fatty acid methyl esters (FAME) of oil and obtained biodiesel were determined by gas chromatography–mass spectroscopy (GC-MS) using an Agilent 5977B series of GC/MS equipped with a SupelcoSP-2560:1531.48227 column of 100 m × 250 m × 0.2 µm dimensions. The oil and biodiesel samples were analyzed at varied temperatures starting from 140 °C to 240 °C following the method described by Lawan et al. [51]. The fuel properties of the produced biodiesel, namely, density at 15 °C, kinematic viscosity at 40 °C and calorific value were determined as per ASTM standards and comparison with the EN14214-established specifications [52].

2.8. Catalysts Recyclability

After the transesterification reaction, the catalysts were separated from the products by centrifugation, washed in acetone and then dried at 200 °C for 120 min. The regenerated catalysts were then re-used in successive transesterification at similar experimental parameters to determine their biodiesel yield and stability in subsequent recycles.

3. Results and Discussion

3.1. Characterization of CaO/CA and NaOH/CA Catalysts

The results of the chemical composition analysis of the synthesized catalysts as determined by XRF are listed on Table 1. The modified catalysts were mainly composed of CaO, MgO, Al_2O_3, Fe, SiO_2, Ti, Mn and P_2O_5 with minor traces of Zn, Sr, Cr and Zr. The presence of the additional metal elements may be due to the purity of the CaO and NaOH used in this experiment. Citate ions have been reported to form strong ionic complexes with metal ions such as Fe^{3+}, Mg^{2+}, Ag^{+}, Ca^{2+} and Zn^{2+} which influence the formation and growth of nanoparticles [53,54].

Table 1. Chemical composition of NaOH/130%CA and CaO/66.5%CA catalysts.

Catalyst	Element Composition (%)								SiO/AL	Basicity (mmol/g)
	MgO	Al_2O_3	SiO_2	P_2O_5	CaO	Mn	Fe	Ti		
NaOH/3%CA-600 °C	72.59	0.17	22.24	0.00	1.32	0.15	1.59	1.33	127.79	1.70
NaOH/66.5%CA-600 °C	71.02	0.17	22.52	0.27	2.30	0.32	2.48	0.76	130.95	2.45
NaOH/130%CA-600 °C	71.96	0.17	22.99	0.12	2.65	0.31	1.21	0.90	133.67	3.61
NaOH/130%CA-300 °C	72.03	0.15	21.38	0.00	2.47	0.29	1.31	1.36	143.46	-
NaOH/130%CA-900 °C	70.68	0.17	23.80	0.00	3.25	0.22	1.15	0.90	144.23	5.33
CaO/3%CA-900 °C	0.20	0.93	0.05	0.80	96.39	0.01	0.18	1.00	0.06	-
CaO/66.5%CA-900 °C	0.11	0.63	0.45	0.81	96.19	0.01	0.00	0.00	0.71	8.70
CaO/130%CA-900 °C	3.41	0.55	0.50	0.97	93.36	0.01	0.18	0.02	0.91	2.65
CaO/66.5%CA-300 °C	3.77	1.83	0.21	0.81	91.40	0.25	0.00	0.00	0.12	0.25
CaO/66.5%CA-600 °C	1.05	1.01	1.02	0.20	96.21	0.00	0.16	0.00	1.01	7.08
CaO	0.00	1.52	0.03	0.26	97.51	0.02	0.17	0.03	0.02	-
CA	86.99	0.00	4.90	0.02	3.91	0.00	2.85	0.15	0.00	-

Increasing the CA wt.% on NaOH resulted in an increased composition of both CaO and SiO_2. On the other hand, increasing the calcination temperatures from 300 to 900 °C resulted in an increase in CaO and SiO_2 composition and a decrease in the composition of MgO, Fe and Ti of the modified NaOH/CA catalyst. When NaOH/130%CA was calcined at 600 °C, it resulted in a maximum biodiesel yield, suggesting that increasing CaO, SiO_2 and MgO composition resulted in increased catalytic activity. These results are in agreement with previous research, where it was reported that incorporating MgO, SrO and CaO on the surface of a catalyst improved the activity of the catalyst in transesterification [55]. For NaOH modified catalysts, high CA wt.% loading and moderate calcination temperatures of 600 °C were the preferred conditions for the catalyst synthesis.

Strangely, increasing CA wt.% loading on CaO resulted in a low percentage composition of CaO, while that of MgO was slightly increased. Moreover, the composition of Al_2O_3 was observed to decrease with an increase in both CA wt. % loading and calcination temperature, suggesting that CA played a role as a dealuminating agent for CaO/CA catalysts. Low calcination temperatures of 300 °C for CaO/CA catalysts resulted in a low biodiesel yield. Moreover, the catalyst showed a low composition of CaO, suggesting that CaO composition played a major role in the activity of the synthesized catalyst. The low catalytic activity of CaO/CA catalysts calcined at 300 °C can be attributed to the fact that $Ca(OH)_2$ decomposes to CaO at temperatures above 600°C [56].

For all the synthesized catalysts, the Si/Al ratio was seen to increase with both an increase in CA wt.% and calcination temperatures, depicting that the synthesis led to dealumination which is linked to a reduction in BrØnsted and Lewis acid site as reported by Vieira et al. [22]. The hydroxyl (Si-(OH)-Al) group has been reported to influence the BrØnsted and Lewis acid site of a catalyst [22,57]. The basicity of all the synthesized catalysts was seen to increase with an increase in calcination temperatures which is in agreement with previous researchers [44,58]. Synthesizing the catalysts with CA decreased the BrØnsted and Lewis acid site, while the basicity was improved which resulted in increased biodiesel productivity.

The FTIR spectra of the functional groups of the modified catalyst is presented in Figure 2. The spectra of CaO and CaO/CA display an O-H bond at 3468 cm^{-1} of the $Ca(OH)_2$ phase, indicating the presence of water molecules on the surface of the catalysts (Figure 2a). The peak corresponding to Ca-O (1590.12 cm^{-1}) was more intense in CaO compared to the synthesized catalysts. This explains the higher composition of CaO in the synthesized catalysts from the XRF results as well as the weaker basic properties of CaO/CA catalysts which may be linked to the lower catalytic activity compared to commercial CaO [56]. The absorbance peaks at 1400.07 cm^{-1} correspond to antisymmetric stretching vibrations C=O due to the presence of carbonate minerals [59,60].

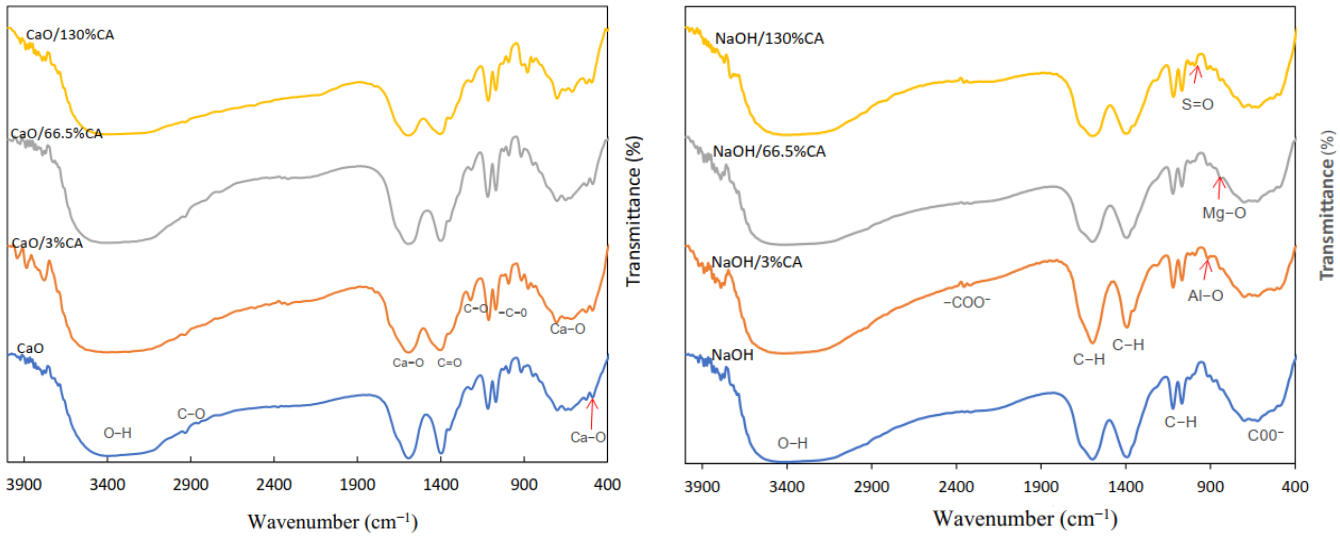

Figure 2. FTIR spectra of different CA loading wt.% on base catalyst: (**a**) CaO/CA; (**b**) NaOH/CA.

Stretching vibrations corresponding to -C-O appear in the region between 1100 cm^{-1} and 900 cm^{-1} indicating that CA was chemically bonded to the surface of CaO [56]. All spectra show strong absorption at 723 cm^{-1} and 454 cm^{-1} which is attributed to the Ca-O bond and the bending mode of $CaCO_3$ vibrations [61]. The peaks intensity of CaO and those of the synthesized catalysts did not change, suggesting that the synthesis connected the CaO surface chemically without modifying the functional group of CaO.

From NaOH/CA spectra (Figure 2b), broad bands are observed between 3438.3 and 3323.14 cm^{-1} which correspond to the stretching vibrations linked with the -OH group. The synthesis resulted in the formation of a covalent bond at 2352.59 cm^{-1} which corresponds to -COO- stretching. This suggests that Na^+ were capped by citrate hydroxyl groups, therefore preventing any change on the surface of the NaOH/CA catalyst when dissolved in methanol [62]. At 1592.95 cm^{-1}, 1390.4 cm^{-1}, 1122.44 cm^{-1} and 1067.16 cm^{-1}, the C-H bonds appear, indicating absorption of citric molecules into the Na surface [63]. A phase shift is observed at 1020.09 cm^{-1} in the NaOH/CA spectra (Figure 2b). Adsorption bands appear at 1029.09 cm^{-1}, 1844 cm^{-1} and 699 cm^{-1} corresponding to S=O, Al-O and Mg-O stretching vibrations, respectively, which is in agreement with the results of XRF [64]. The characteristics bands at 651.9 cm^{-1}, 621.1 cm^{-1} and 479.47 cm^{-1} of the hexagonal phases of trisodium citrate were observed for all the catalysts. In all spectra (Figure 2a,b), the synthesis is seen to result in active vibrations at the fingerprints region showing vinyl compounds and aromatic bonds between 400 and700 cm^{-1} [65].

Surface Morphology and Crystalline Structure of Synthesized Catalysts

The scanning electron microscopy (SEM) micrographs of the synthesized catalysts are presented in Figure 3. The micrographs of the CaO/CA catalysts showed smaller particle size and more rounded edges compared to those of the parent CaO (Figure 3a). The particles of CAO/3%CA showed well-defined shape with greater particle dispersion compared to CaO/66%CA and CaO/130%CA. The micrographs of CaO/66%CA and CaO/130%CA showed amorphous-like particles with rounded shapes, and their edges were not well defined. The best transesterification activity was attained with CaO/3%CA indicating that a low percentage of CA resulted in greater dispersion of CaO species and a more refined particle size of the modified catalyst.

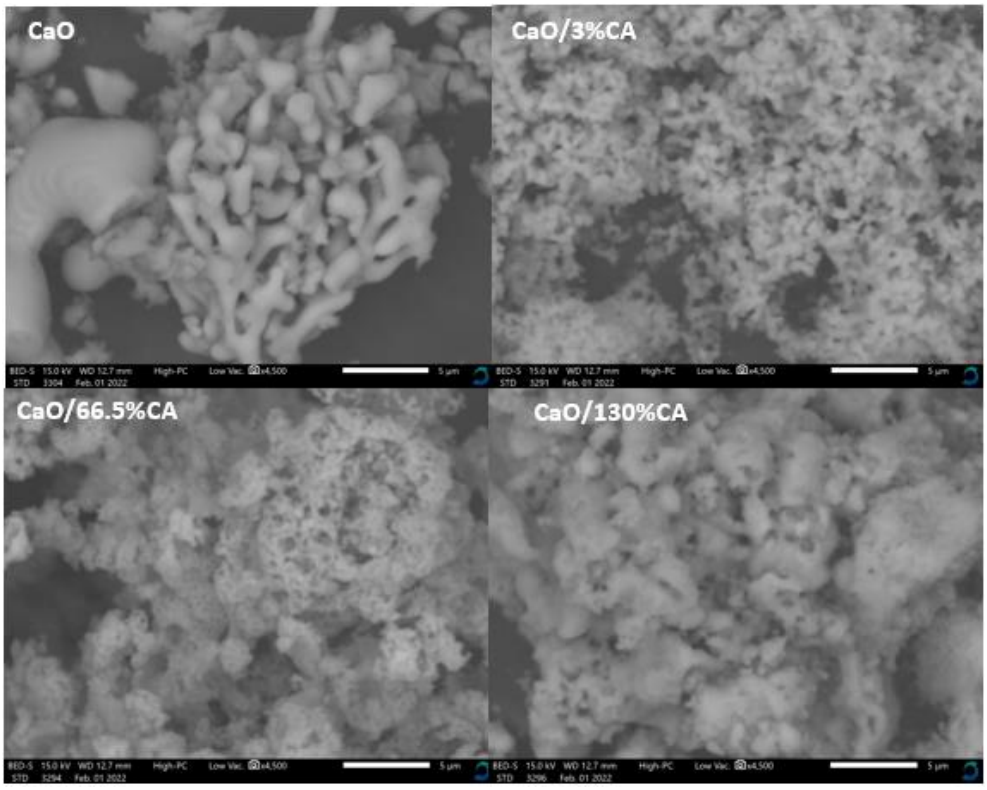

(**a**)

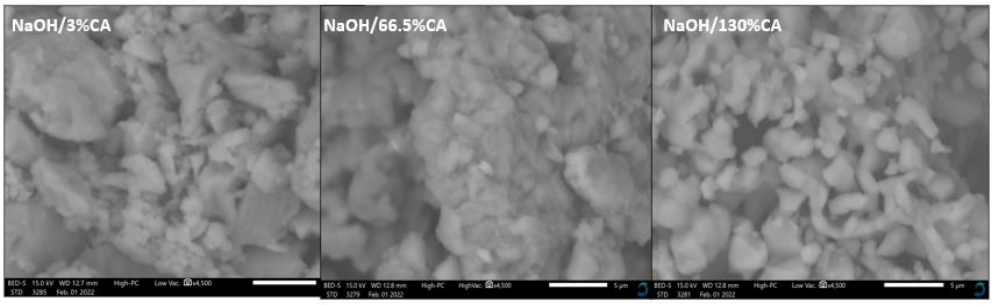

(**b**)

Figure 3. SEM micrographs of the catalysts with varied wt.% loading of citric acid: (**a**) CaO/CA catalysts; (**b**) NaOH/CA catalysts.

On the other hand, NaOH/3%CA micrographs display rough edges. However, as the concentration of citric acid was increased to 66.5 wt.%, the modified catalyst displayed fine and smoother edges (Figure 3b). When CA wt.% was further increased to 130%, the particles displayed well-formed shapes, indicating successful crystal growth during the precipitation stage. NaOH/130%CA is seen to have well-formed particle distribution indicating that high CA loading on NaOH resulted in improved dispersion of NaOH species which explains the increased catalytic activity. A study by Meng et al. [24] also reported that the addition of citric acid increased the dispersion of Mo species, thus improving catalytic activity of MoO_3/Al_2O_3 in methanation.

Synthesizing the catalysts with CA resulted in a reduced apparent particle size of the catalysts (Table 2) and refined particle dispersion. The contradicting effects of CA wt.% on NaOH/CA and CaO/CA catalyst particle dispersion and refinement may be attributed to the preparation method. High CA wt.% was effective for the precipitation of NaOH/CA crystals, while CA weakly attached to the CaO surface in the impregnation process. The results show that CA is more likely to bind to Na^+ compared to Ca^{2+}.

Table 2. XRD Structural properties and catalytic activity of synthesized catalysts.

Catalyst	Crystallite Size (nm)	Crystallinity (%)	Relative Cross Section Size (μm) *	Biodiesel Yield (%)
NaOH/130%CA-300 °C	86.35	52.65	1.94	66.5
NaOH/130%CA-600 °C	56.98	69.00	1.46	93
NaOH/130%CA-900 °C	54.73	63.53	1.44	88.5
CaO/66.5%CA-300 °C	56.80	5.76	1.78	52.5
CaO/66.5%CA-600 °C	49.71	64.70	1.35	90.5
CaO/66.5%CA-900 °C	56.80	67.09	1.41	91.5
CaO	70.58	64.92	1.6	92.05

* Measurements from SEM at 20 μm.

The XRD diffractograms of the synthesized CaO catalysts are depicted in Figure 4. The spectra patterns of the CaO/CA catalysts displayed sharp peaks that correspond to CaO at 2θ values of 29.75°, 32.74°, 37.86°, 54.82°, 64.74° and 68.02°. These patterns are similar to those of the modified CaO nanocatalyst [31,66]. At lower calcination temperatures of 300 °C, the diffractogram of the modified catalyst was highly amorphous which accounts for the low crystallinity and low biodiesel yield from the catalyst (Table 2). At higher calcination temperatures of 600 °C, the peaks intensity of CaO phases increased and were comparable to those of commercial CaO. This is in agreement with the XRF results, where the composition of the CaO was seen to increase with the increase in calcination temperature. The percentage crystallinity of the CaO/CA catalysts calcined at 600 °C and 900 °C was 64.70% and 76.09%, respectively. These results are comparable to those of commercial CaO with 64.93%. The calculated crystalline size of the CaO was 70.58 nm which was greater than that of the synthesized catalysts (Table 2). This is in agreement with the SEM micrographs as well as the relative size estimation. The results compare to a previous study by Wong et al. [58] where the crystallite size of CaO was reported to be 66.5 nm when calcined at 700 °C.

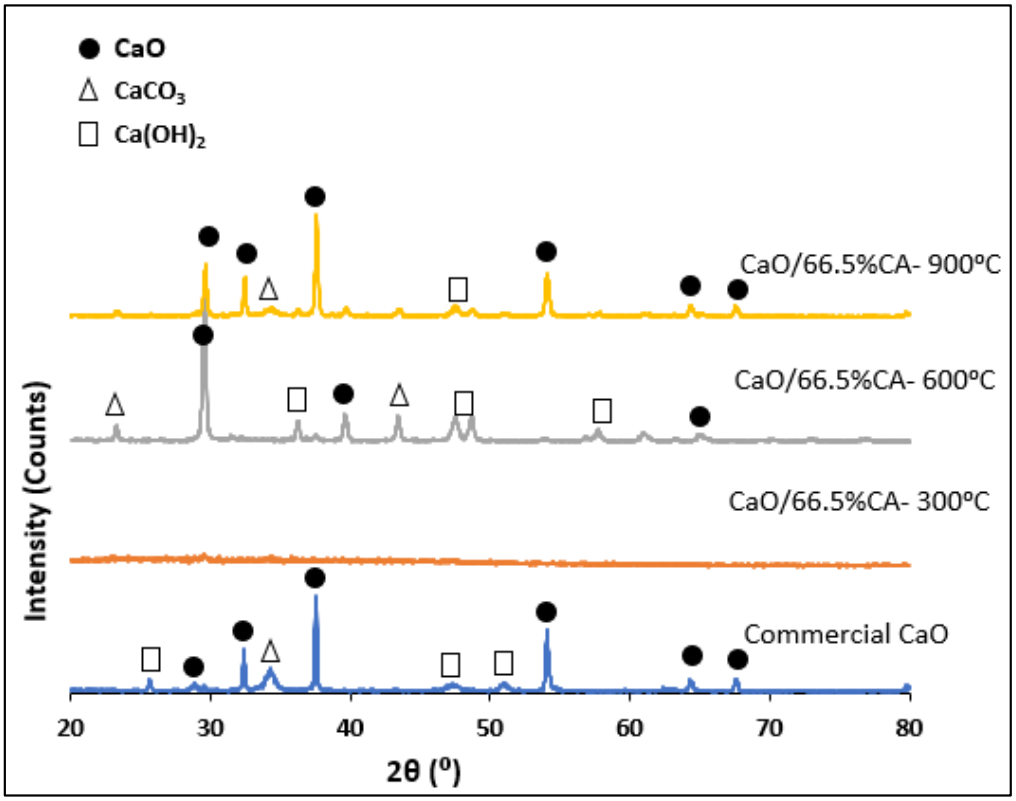

Figure 4. RXD pattern of CaO/CA and commercial CaO catalysts.

The XRD patterns of NaOH/CA catalysts showed several diffraction peaks indicating the presence of Na_2O, $NaOH{\cdot}H_2O$, $NaAlSiO_4$, SiO_2 and MgO in hydrated and anhydrous form Figure 5.

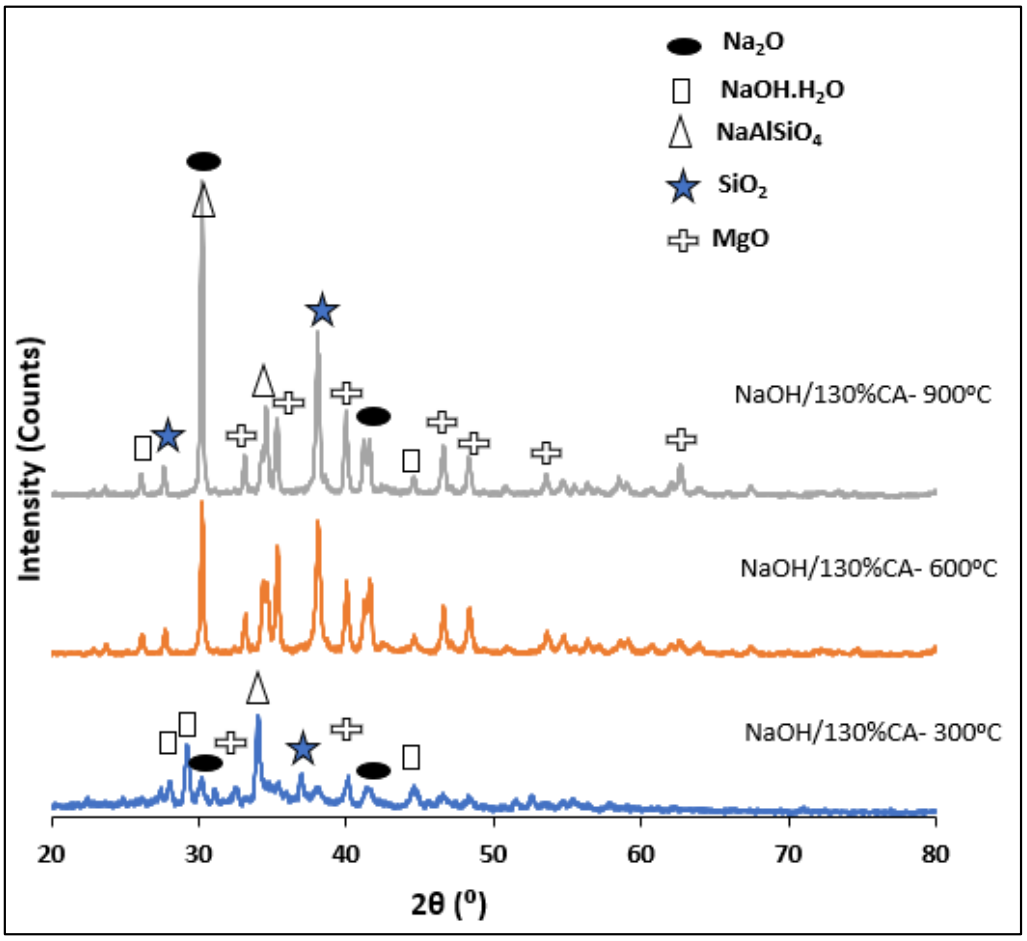

Figure 5. RXD pattern of NaOH/CA catalysts.

The peaks corresponding to the Na_2O phase were seen to intensify with an increase in calcination temperature which was inconsistent with the decrease in crystallite sizes and the increase in biodiesel yield as shown in Table 2. Moreover, an increase in calcination temperatures resulted in an increase in SiO_2 peak intensity which is in agreement with previously discussed XRF results. These results suggest that the NaOH successively reacted with the CA resulting in the formation of nitrites with aluminates and silicates. This is in accordance with previous studies on trisodium citrate and NaOH/alumina catalysts [67,68].

3.2. Central Composite Design (CCD) Analysis for Biodiesel Yield

A summary of the three block, (set1, set2 and set3), four factor, three level, full factorial CCD matrix is presented in Table 3. The design provided 30 experimental runs for each synthesized catalyst.

The data were analysed using ANOVA and showed that the RSM model used in this study was statistically significant (p = 0.0022, r = 0.9235, R^2 = 0.8529 for CaO/CA and p = 0.0027, r = 0.9606, R^2 = 0.8476 for NaOH/CA catalyst) in representing the relationship between the independent and dependent variables of the quadratic Equation (3). The coded equation showed positive coefficients of X3 and X4 for the CaO catalyst (Equation (4)) and X1, X3 and X4 for the NaOH/CA catalysts (Equation (5)), indicating that their variation had an effect on the response (biodiesel yield). For the CaO/CA catalysts, the CA wt.% and the calcination temperature were the two variables that

showed significant ($p < 0.05$) influence on biodiesel yield. While for the NaOH/CA catalyst, the CA wt.%, calcination temperature and the synthesis temperature influenced the catalyst's activity in transesterification. The lack of fit F-values of 1.42 and 5.01 for CaO/CA and NaOH/CA, respectively, were not significant, indicating the model's goodness of fit. The prediction model of the biodiesel yield using the modified catalyst positively correlated with the actual experiment is shown by the plots in Figure 6. This shows that the determined coefficients of regression presented by Equations (4) and (5) provided relevant descriptions of the experimental data.

$$\begin{aligned} Y = \quad & +78.92 - 5.88X_1 - 0.28X_2 + 18.69X_3 + 4.22X_4 - 0.14{X_1}^2 - 4.16{X_2}^2 \\ & -8.16{X_3}^2 - 0.82{X_4}^2 - 1.63X_1X_2 - 1.05 + 1.73X_1X_3 - 0.14X_1X_4 - 1.73X_2X_3 \\ & +0.9X_2X_4 - 0.49X_3X_4 \end{aligned} \quad (4)$$

$$\begin{aligned} Y = \quad & +83.84 + 9.73X_1 - 4.07X_2 + 5.55X_3 + 5.94X_4 + 1.97{X_1}^2 - 9.57{X_2}^2 \\ & -12.63{X_3}^2 - 2.55{X_4}^2 - 0.31X_1X_2 + 0.58X_1X_3 + 1.37X_1 - 1.08X_40.2X_2X_3 \\ & -1.82X_2X_4 - 2.73X_3X_4 \end{aligned} \quad (5)$$

Table 3. Central composite design matrix for BSFL biodiesel yield.

Std	Block	Run	Independent Variables				Biodiesel Yield (%)	Biodiesel Yield (%)
			X1:	X2:	X3:	X4:		
			CA Loading (wt.%)	Synthesis Temperature (°C)	Calcination Temperature (°C)	Calcination Time (Minutes)	CaO/CA	NaOH/CA
14	Set 1	1	130	80	900	240	78.25	86.55
15	Set 1	2	3	200	900	240	88.55	50.2
2	Set 1	3	130	80	300	90	48.2	65.5
3	Set 1	4	3	200	300	90	68.15	48.55
12	Set 1	5	130	200	300	240	50	75.15
5	Set 1	6	3	80	900	90	88.55	60
9	Set 1	7	3	80	300	240	60	58.5
18	Set 1	8	66.5	140	600	165	78.25	80
8	Set 1	9	130	200	900	90	75.5	76.44
17	Set 1	10	66.5	140	600	165	60.25	80.75
1	Set 2	11	3	80	300	90	42.5	52.16
4	Set 2	12	130	200	300	90	38	70
10	Set 2	13	130	80	300	240	40.5	88.25
16	Set 2	14	130	200	900	240	90	74
6	Set 2	15	130	80	900	90	90.5	86.66
19	Set 2	16	66.5	140	600	165	90	80
7	Set 2	17	3	200	900	90	90	55.05
20	Set 2	18	66.5	140	600	165	75.25	89.5
13	Set 2	19	3	80	900	240	91.5	60
11	Set 2	20	3	200	300	240	58	50.55
25	Set 3	21	66.5	140	0	165	0	0
29	Set 3	22	66.5	140	600	165	91.5	92.24
22	Set 3	23	193.5	140	600	165	56.15	93.15
21	Set 3	24	-60.5	140	600	165	88.5	70.15
23	Set 3	25	66.5	20	600	165	62.5	45.52
24	Set 3	26	66.5	260	600	165	50	25.5
26	Set 3	27	66.5	140	1200	165	80.5	46.5
27	Set 3	28	66.5	140	600	15	48.11	35.15
30	Set 3	29	66.5	140	600	165	78.25	80.55
28	Set 3	30	66.5	140	600	315	91.05	92

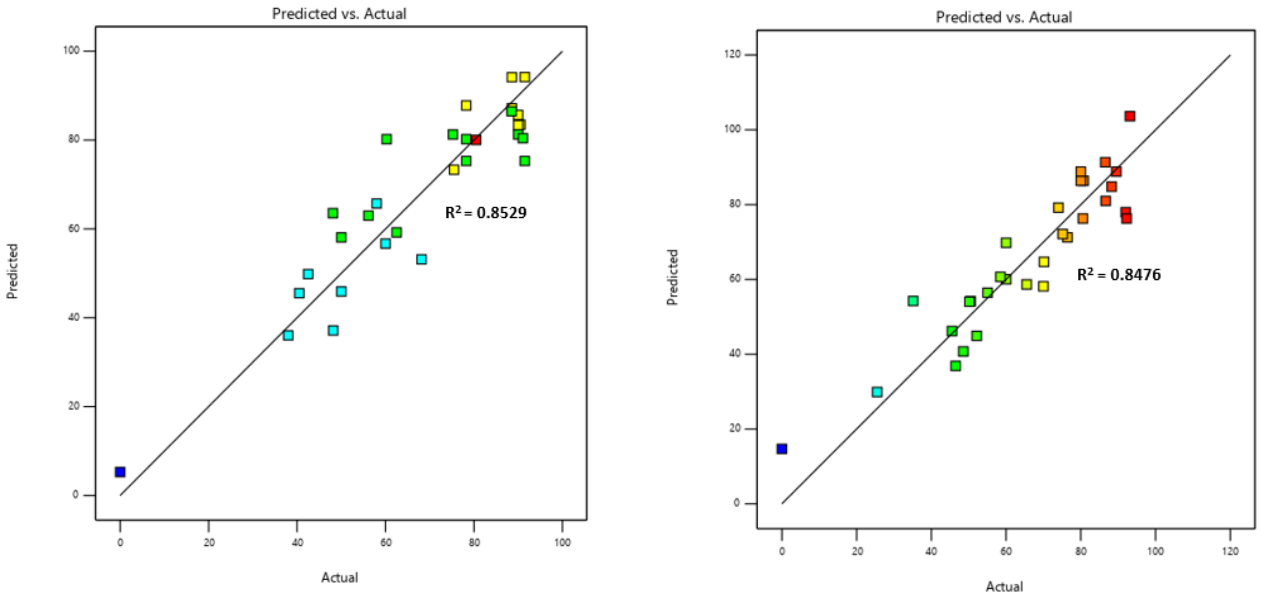

(**a**) (**b**)

Figure 6. Plots of prediction against actual biodiesel yield: (**a**) CaO/CA; (**b**) NAOH/CA.

For model results verification of optimum conditions by experiment, when NaOH was precipitated with 100 wt.%CA at 80 °C and calcined at 600 °C for 4 h, it resulted in a biodiesel yield of 93.08%, ±1.31, while the model predicted a yield of 95.12%. Likewise, when CaO was impregnated with 40 wt.%CA at 140 °C and calcined at 800 °C for 3 h, it yielded 90.35.%, ±1.99, biodiesel, while the prediction was 91.18%. This showed that there was a good correlation between the experimental and predicted biodiesel yield results. The results showed the ability of synthesizing NaOH and CaO with citric acid to form modified catalysts with high activity in transesterification.

3.3. Assessment of Catalytic Performance in Transesterification of BSFL Oil

3.3.1. Effects of Citric Acid Loading wt.% on CaO and NaOH on Biodiesel Yield

In the absence of a catalyst, the transesterification of BFSL oil into biodiesel did not occur, indicating that for the reaction to shift forward to form FAME, a catalyst must be present. Figure 7 shows the effect of the CA loading weight on transesterification performance of the synthesized catalysts.

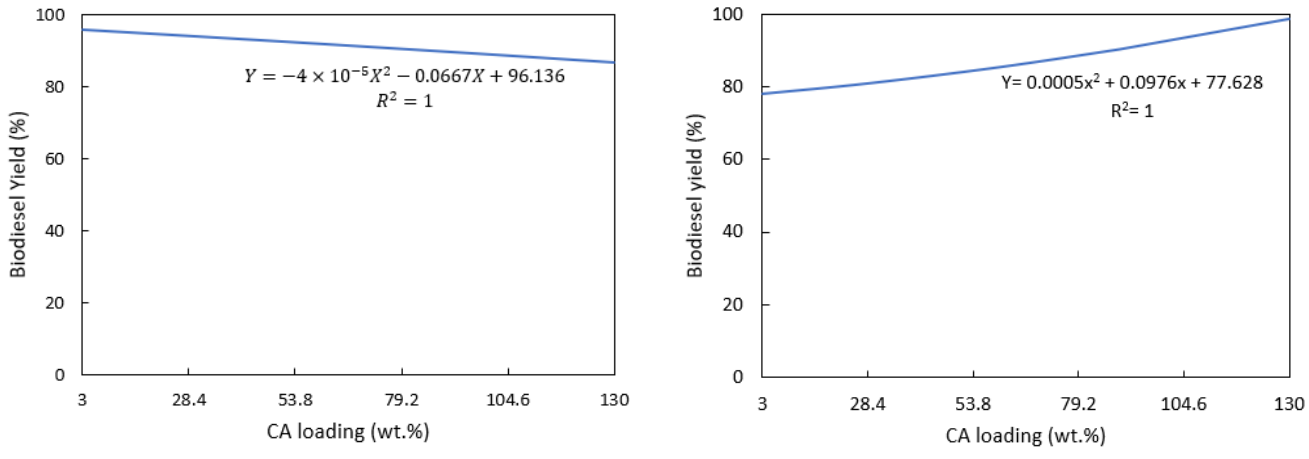

(**a**) (**b**)

Figure 7. Effects of the citric acid loading wt.% on biodiesel yield: (**a**) CaO/CA; (**b**) NaOH/CA.

Synthesizing CaO with citric acid attained a maximum biodiesel yield of 94.25%, ±1.6, as illustrated in Figure 7a. At a lower CA loading of 3–50 wt.%, the modified catalyst resulted in a biodiesel yield above 90%. However, at a higher CA loading of more than 50 wt.%, biodiesel yield decreased gradually. As previously seen from the SEM images, high wt.% of CA on CaO inhibits the dispersion of particles; therefore, it has the tendency to decrease the activity of the catalysts. On the other hand, biodiesel yield increased with CA wt.% on NaOH attaining a maximum yield of 94%, ±3.5, at 130 wt.% (Figure 7b). In their experiments, Macina et al. [39] used high wt.% loading of citric acid on NaOH in preparation for a carbon-dot catalyst with CA and NaOH. However, the effects of citric acid on the modified catalyst were not discussed in the study. NaOH requires a high concentration of citric acid for effective crystallization during the precipitation step. A high wt.% of CA on NaOH was also observed to increase the particle dispersion from SEM images, thus increasing the activity of the catalyst.

3.3.2. Effects of Synthesis Temperatures on Biodiesel Yield

The synthesis temperature had great impact on NaOH/CA compared to CaO/CA catalysts (Figure 8). NaOH/CA catalysts were more active when synthesized at lower temperatures compared to CaO/CA (Figure 8a). The optimum synthesis temperatures for the two catalysts were 100 °C and 140 °C, respectively. The reaction between NaOH with CA for precipitation is exothermic, and maintaining the temperature at 80 °C resulted in a higher crystal yield, indicating that for successful precipitation of sodium hydroxide with citric acid, it is important to maintain the synthesis temperature at the range of 80–100 °C. Experiments have also reported the possibility of precipitation of NaOH with CA at ambient temperatures [40]. The CaO/CA catalysts required a higher synthesis temperature (140 °C) for impregnation to be completed (Figure 8b). However, very high impregnation temperatures of above 170 °C resulted in decreased biodiesel yield which could be attributed to the fact that the solution dried up very fast, hindering the complete synthesis of the precursors with CA.

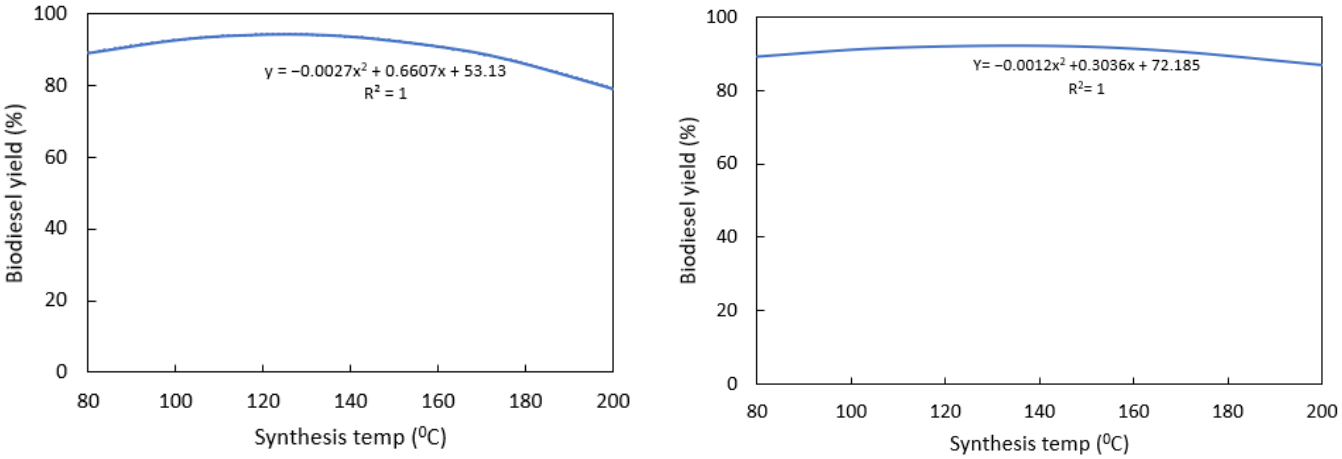

(**a**) (**b**)

Figure 8. Effects of synthesis temperatures on biodiesel yield: (**a**) NaOH/CA; (**b**) CaO/CA.

3.3.3. Effect of Calcination Temperatures and Time on Biodiesel Yield

The catalytic activity of CaO/CA increased with an increase in calcination temperatures, while that of NaOH/CA curtailed when calcination temperatures were raised beyond 650 °C. At low calcination temperatures below 600 °C, CaO/CA catalysts resulted in low biodiesel yield. This was attributed to the low composition of CaO due to the presence of $Ca(OH)_2$ and $CaCO_3$ at low calcination temperatures [58]. At high calcination temperatures, CaO/CA resulted in increased biodiesel yield (Figure 9a) attaining a maximum yield of 90.5% when calcinated at 800 °C, indicating that high calcination temperatures within the

range of 700–800 °C were the most favourable for the synthesis of CaO/CA catalysts. These results are in agreement with results from a previous study by Wong et al. [58] who reported that CaO/NB_2O_5 resulted in high biodiesel yield when calcined at 600 °C. The authors observed that low calcination temperatures promoted the formation of CO_2 and moisture inhibiting the catalyst activity. On the other hand, very high calcination temperatures caused crystals to sinter and agglomerate. Referring to the NaOH/CA catalyst, increasing the calcination temperatures beyond 800 °C resulted in decreased catalytic activity as demonstrated in Figure 9b. A maximum biodiesel yield of 93.15% was attained when the catalyst was calcined at 600 °C for four hours.

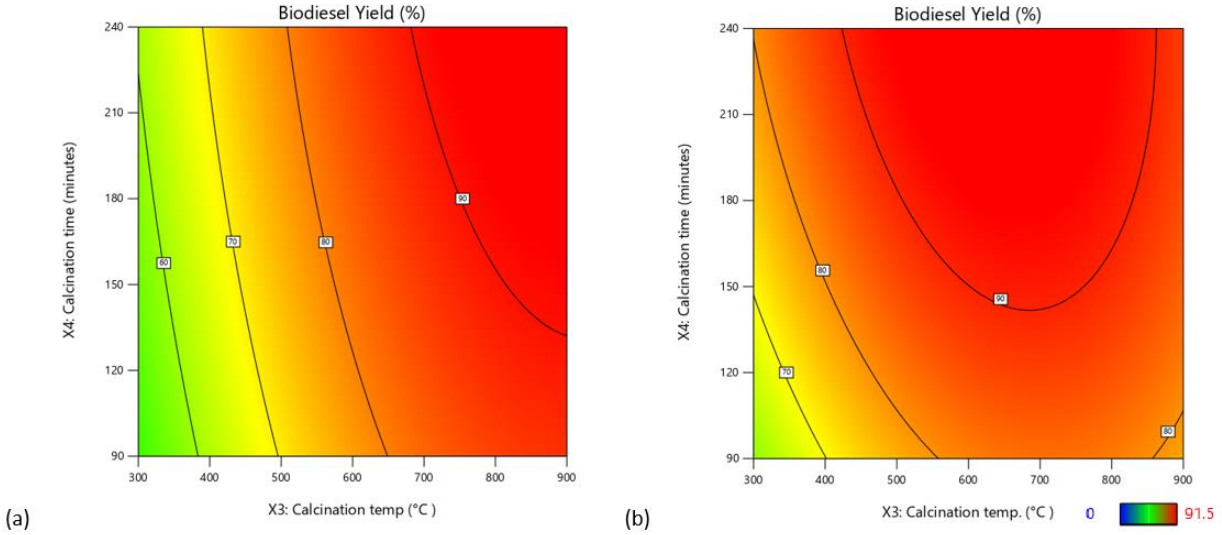

Figure 9. Effect of calcination temperatures and time on biodiesel yield: (**a**) CaO/CA; (**b**) NaOH/CA.

The calcination temperature and CA wt.% were the two main independent variables that exhibited pronounced variation in biodiesel yield as shown by the three-dimensional and contour diagrams presented in Figure 10. For the CaO/CA catalyst, low CA wt.% (3–50 wt.%) and high calcination temperatures (above 700 °C) were the most favourable conditions for high biodiesel yield (Figure 10a), while for the NaOH/CA, a high CA wt.% (100–130 wt.%) and lower calcination temperatures (500–600 °C) resulted in high biodiesel yield (Figure 10b). Therefore, the optimum conditions were 900 °C and 46 wt.% for CaO/CA, and 600 °C and 130 wt.% for NaOH/CA, respectively.

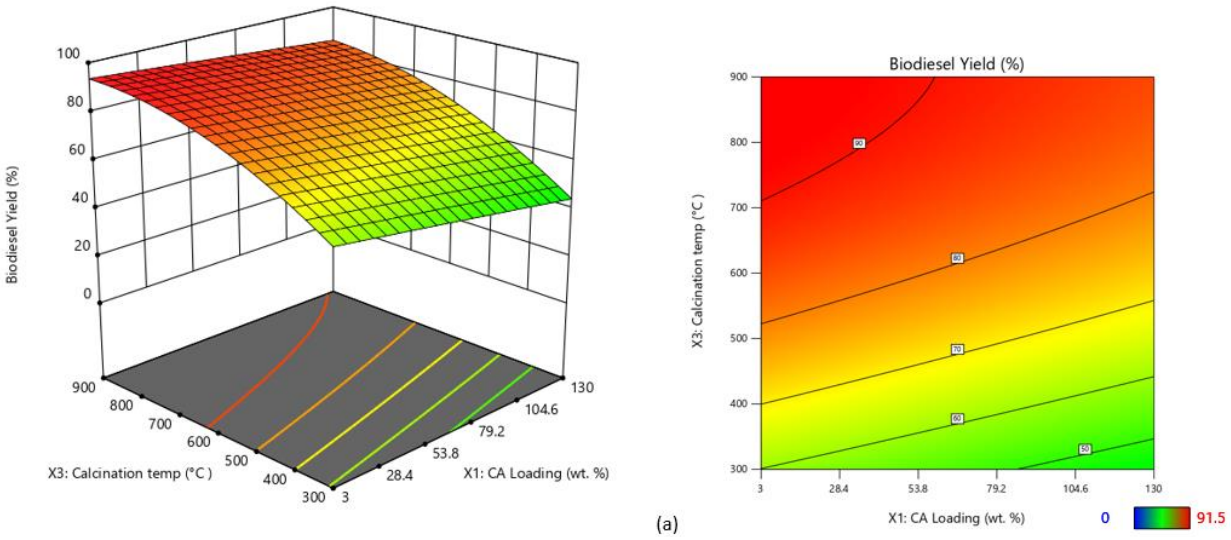

Figure 10. *Cont.*

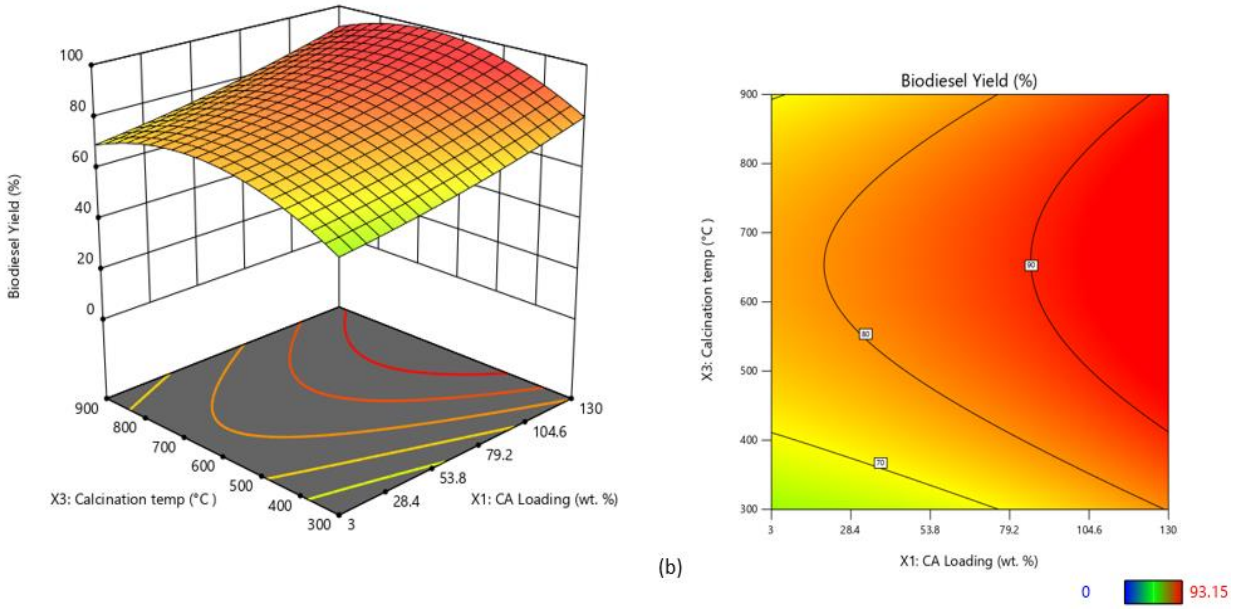

Figure 10. Three-dimensional surface and contour plots of biodiesel yield from the synthesized catalysts: (**a**) CaO/CA; (**b**) NaOH/CA.

3.4. Composition and Fuel Properties of BSFL-Based Oil and Biodiesel

Results of the chemical composition of biodiesel derived from BSFL were determined by GCMS as shown in Table 4 and Figure 11, respectively. The produced biodiesel was mainly composed of lauric, palmitic, stearic and oleic acid with a high concentration of saturated fatty acids (73.34–74.78%). The biodiesel composition profile of NaOH/CA and CaO/CA was similar to that of the CaO catalyst, indicating the effectiveness of the synthesis in transesterification.

Table 4. Fatty acids composition of BSFL biodiesel.

Fatty Acid	The Numbers Denote the Number of Carbons and Double Bonds	Relative Content (%)		
		NaOH/CA	CaO/CA	CaO
Nanoic acid	C9:0	0.02%	0.03%	0.03%
Dodecane	_	0.08%	0.17%	0.12%
Caproic acid	C10:0	0.66%	0.37%	0.66%
Lauric acid	C12:0	36.00%	41.22%	41.29%
Myristic acid	C14:0	11.92%	11.47%	12.33%
Pentadecanoic acid	C15:0	0.08%	0.08%	0.09%
Palmitoleic acid	C16:1	0.45%	0.12%	0.11%
Palmitic acid	C16:0	21.28%	18.36%	16.12%
Heptadecanoic acid	C17:0	0.14%	0.35%	0.44%
Oleic acid	C18:1	25.70%	24.61%	24.00%
Stearic acid	C18:0	3.12%	2.46%	3.66%
Linoleic acid	C18:2	0.46%	0.63%	1.03%
Linolenic acid	C18:3	0.05%	0.07%	0.08%
Nonadecanoic acid	C19:0	0.04%	0.06%	0.04%
Saturated Fatty Acids (SFA)		73.26%	74.40%	74.66%
Monounsaturated Fatty Acids (MUFA)		26.15%	24.73%	24.11%
Polyunsaturated Fatty Acids (PUFA)		0.51%	0.70%	1.11%

The FAME profile was in agreement with previous studies where the biodiesel from BSFL has been reported to have a high composition of saturated fatty acids, indicating the potential to produce high quality biodiesel [69–71]. A high concentration of saturated fatty acids results in high oxidative stability of produced biodiesel, while biodiesel with high polysaturated fatty acids is prone to suffer oxidation [72]. Biodiesel from BSFL has high

saturated fatty acids; hence, it may have higher oxidation stability in comparison to energy crops such as rapeseed [69].

The FTIR spectra of oil and biodiesel derived from BSFL is presented in Figure 12. Broad and strong O-H bonds were observed at 3480.06 cm^{-1}, indicating the presence of moisture in the oil and biodiesel [73]. Strong absorbance peaks were observed at 2926 cm^{-1} and 2855 cm^{-1} which correspond to a C-H antisymmetric stretching vibration of methyl and methylene groups, indicating a high composition of saturated fatty acids in oil and biodiesel from BSFL [74]. These results are in agreement with the previously discussed GCMS results. The peak at 1741.76 cm^{-1}, corresponding to C=O stretching vibrations of the functional group of esters, is more intense in the spectra of oil and that of biodiesel produced by CA compared to that of biodiesel produced by NaOH/CA, indicating the presence of carboxylic acids [75].

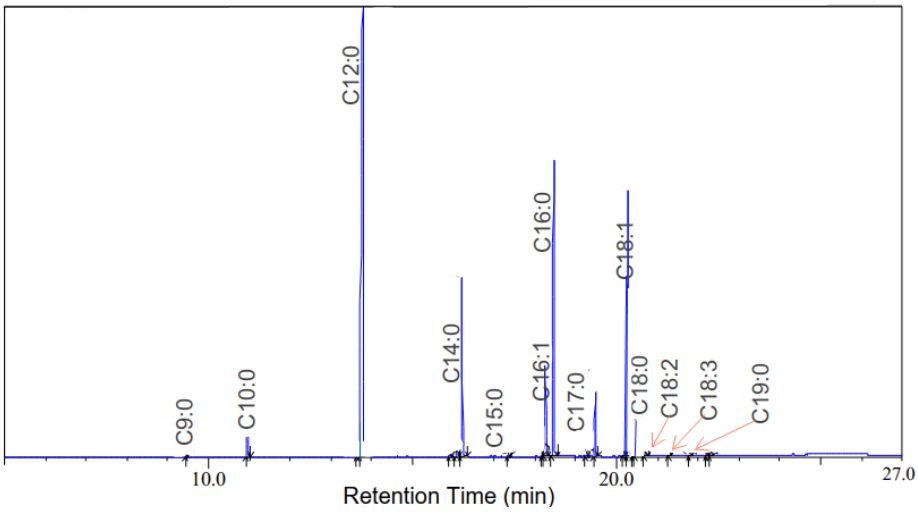

Figure 11. GCMS chromatographs of fatty acids and FAME derives from BSFL biodiesel.

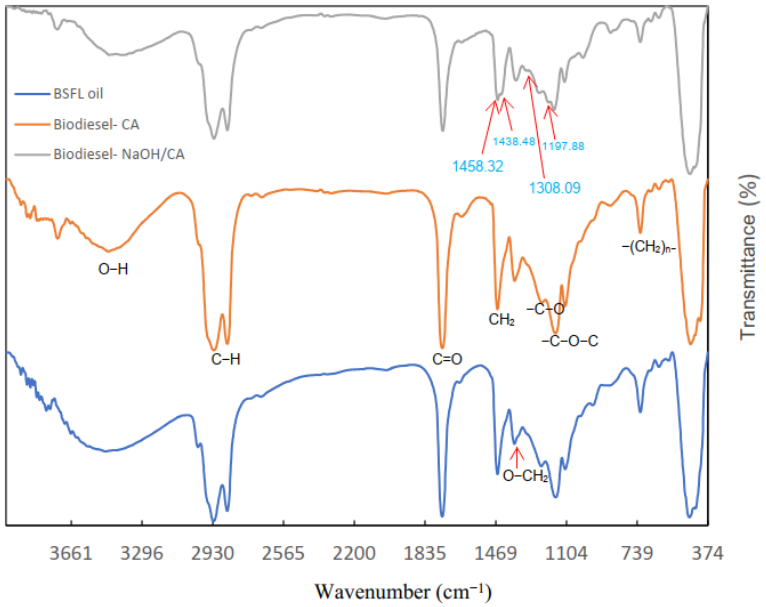

Figure 12. Comparison of FTIR spectra of BSFL-derived oil and biodiesel.

The most distinctive feature in the spectra of oil and biodiesel is seen between 1500 cm^{-1} and 1000 cm^{-1}. Peaks were observed at 1458.32 cm^{-1}, 1438.48 cm^{-1} and 1197.88 cm^{-1} which correspond to CH_2, CH_3 and O-CH_3 of the methyl ester groups in the spectra of the biodiesel produced by NaOH/CA only [76]. Second, a scissoring split of the -C-H group at 1458.32 and the asymmetric bend corresponding to methyl ester

moiety in the spectra of Biodiesel produced using NaOH/CA confirm the presence of methyl esters that are absent in the spectra of BSFL oil and biodiesel produced using CA as the catalyst [7]. There was no noticeable difference between the spectra of BSFL oil and that of biodiesel produced using CA catalysts (biodiesel-CA), indicating that complete transesterification of the BSFL oil into biodiesel did not take place when CA was used as a catalyst. This shows that CA could not be effectively used as a catalyst in transesterification of BSFL oil under the same conditions as NaOH/CA, CAO/CA and CaO. Moreover, it was difficult to recover CA for recycling after the transesterification process. These results show the potential of BSFL in biodiesel production as well as the ability of the modified catalysts in transesterification of oil into biodiesel.

The fuel properties of the biodiesel produced using NaOH/CA and CaO/CA catalysts (Table 5) met the European biodiesel standards, EN14241, and are comparable to those previously reported by Li et al. [69], proving the effectiveness of the modified catalysts in transesterification of BSFL oil into biodiesel.

Table 5. Properties of BSFL biodiesel.

Properties	EN14214	Biodiesel from BSFL
Density (kg/m^3)	860–900	862.2–868.4
Kinematic viscosity at 40 °C (mm^2/s)	2.5–6.0	4.2–5
Acid number (mg KOH/g)	0.5	0.31–0.44
Refractive index 40 °C	_	1.4535–1.4461
Calorific value (Mj/kg)	_	37.8–39.14
Polyunsaturated methyl esters	<1%	0.51–1.11%

3.5. Performance of The Synthesized Catalysts in Successive Reuse Cycles

Both the CaO/CA and the NaOH/CA attained biodiesel yield above 70% (Figure 13) in the first four cycles. The modified catalysts were easy to separate from the biodiesel product for recycling, showing their effectiveness in biodiesel production. Difficulty to separate and clean the catalysts was noticed in the fourth to fifth cycle, and biodiesel yield was significantly reduced after the fifth cycle. The catalysts deactivation may be attributed to thermal degradation causing the loss of an active site over repeated use due to sintering. CaO demonstrated high reactivity in the first cycle; however, biodiesel yield dropped below 70% after the second cycle. This may be attributed to the leaching effect of CaO [77,78]. CaO/CA exhibited higher yields by 13.4%, 20%, 23.6% and 49.4% in the second, third, fourth and fifth cycles, respectively, compared to CaO. This may be due to slow leaching of the CaO/CA catalyst during subsequent transesterification reactions. From an earlier study, it was reported that when CaO is synthesized with a metal oxide, the modified catalyst exhibited insignificant leaching in biodiesel production [41].

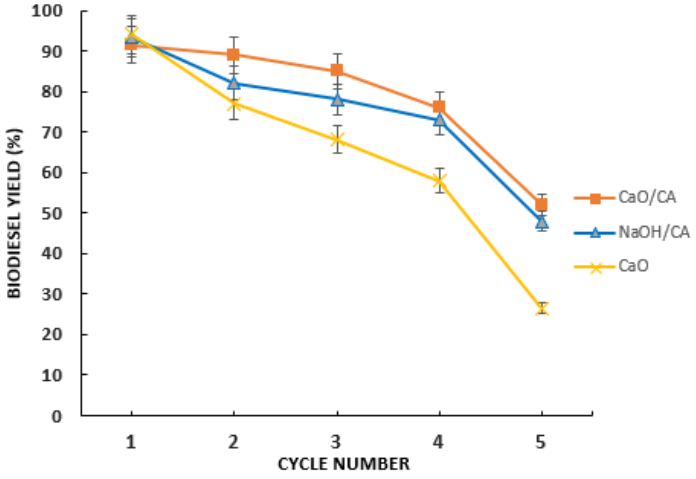

Figure 13. Biodiesel yield with different recycles of the catalyst in transesterification of BSFL oil.

4. Conclusions

This research investigated the effect of synthesizing NaOH and CaO with CA on the activity of the catalyst in transesterification of oil from BSFL fed on kitchen waste. On its own, CA was a poor catalyst for transesterification of BSFL oil. Moreover, it was difficult to recover and separate CA and the products of transesterification.

When NaOH was synthesized with citric acid at 130 wt.%, a synthesis temperature of 80 °C and a calcination temperature of 600 °C for 4 h, it formed a heterogenous catalyst with high biodiesel yield of up to 93.25%. CA was covalently bonded with Na, forming a modified catalyst with improved composition of Mn, CaO and SiO_2. Higher CA wt.% loading on NaOH improved particle dispersion and crystallinity and resulted in smaller crystallite size which improved the catalytic activity of the modified catalyst. Moreover, NaOH/CA was easy to separate from biodiesel, making transesterification process less tedious.

On the other hand, CaO is a heterogenous catalyst with a high biodiesel yield of 92.05%. However, when recycled, the biodiesel yield greatly reduced after the second cycle. Synthesizing CaO with citric acid at 3 wt.%CA, an impregnation temperature of 140 °C and a calcination temperature of 900°C for 4 h formed a modified catalyst with a biodiesel yield of 90.5%. A low CA wt.% on CaO improved particle dispersion, while a high CA wt.% resulted in reduced CaO composition and agglomeration of particles. A very high CA wt.% on CaO showed reduced catalytic activity of the modified catalyst. The modified CaO/CA catalyst displayed smaller crystallite size and was more stable in subsequent reuse cycles than the parent CaO by more than 13%. Both CaO/CA and NaOH/CA could be recycled up to four times while maintaining biodiesel yield above 70%.

This study contributes to the development of catalysts for biodiesel production from waste-related resources. It demonstrates the possibility of synthesizing transesterification catalysts with CA (an organic acid) for biodiesel production from BSFL. Future studies should investigate whether synthesizing catalysts with citric acid can inhibit deactivation and leaching of a heterogenous catalyst in subsequent reuse cycles.

Author Contributions: Conceptualization, methodology, data curation, writing—original draft, L.K.K.; conceptualization, supervision, formal analysis, writing—review and editing P.G.H., J.M.R. and B.B.G.; project administration, J.M.R.; investigation, B.B.G.; funding acquisition, P.G.H. All authors have read and agreed to the published version of the manuscript.

Funding: Authors would like to specially thank Africa-ai-Japan for the financial support under grant number JFY2020/21.

Institutional Review Board Statement: Not applicable.

Informed Consent Statement: Not applicable.

Data Availability Statement: Not applicable.

Conflicts of Interest: The authors declare no conflict of interest.

References

1. Chiaramonti, D.; Talluri, G.; Scarlat, N.; Prussi, M. The challenge of forecasting the role of biofuel in EU transport decar-bonisation at 2050: A meta-analysis review of published scenarios. *Renew. Sustain. Energy Rev.* **2021**, *139*, 110715. [CrossRef]
2. Avinash, A.; Murugesan, A. Economic analysis of biodiesel production from waste cooking oil. *Energy Sources Part B Econ. Plan. Policy* **2017**, *12*, 892–894. [CrossRef]
3. Melero, J.A.; Sánchez-Vázquez, R.; Vasiliadou, I.A.; Martínez Castillejo, F.; Bautista, L.F.; Iglesias, J.; Morales, G.; Molina, R. Municipal sewage sludge to biodiesel by simultaneous extraction and conversion of lipids. *Energy Convers. Manag.* **2015**, *103*, 111–118. [CrossRef]
4. Davis, R.; Aden, A.; Pienkos, P.T. Techno-economic analysis of autotrophic microalgae for fuel production. *Appl. Energy* **2011**, *88*, 3524–3531. [CrossRef]
5. Karmee, S.K.; Linardi, D.; Lee, J.; Lin, C.S.K. Conversion of lipid from food waste to biodiesel. *Waste Manag.* **2015**, *41*, 169–173. [CrossRef]
6. Wong, C.Y.; Rosli, S.S.; Uemura, Y.; Ho, Y.C.; Leejeerajumnean, A.; Kiatkittipong, W.; Cheng, C.K.; Lam, M.-K.; Lim, J.W. Potential protein and biodiesel sources from black soldier fly larvae: Insights of larval harvesting instar and fermented feeding medium. *Energies* **2019**, *12*, 1570. [CrossRef]

7. Wang, C.; Qian, L.; Wang, W.; Wang, T.; Deng, Z.; Yang, F.; Xiong, J.; Feng, W. Exploring the potential of lipids from black soldier fly: New paradigm for biodiesel production (I). *Renew. Energy* **2017**, *111*, 749–756. [CrossRef]
8. Srivastava, N.; Srivastava, M.; Mishra, P.K.; Gupta, V.K. *Substrate Analysis for Effective Biofuels Production*; Springer Nature: Berlin/Heidelberg, Germany, 2020.
9. Baskar, G.; Aiswarya, R. Trends in catalytic production of biodiesel from various feedstocks. *Renew. Sustain. Energy Rev.* **2016**, *57*, 496–504. [CrossRef]
10. Aransiola, E.F.; Ojumu, T.V.; Oyekola, O.O.; Madzimbamuto, T.F. A review of current technology for biodiesel production: State of the art. *Biomass Bioenergy* **2015**, *61*, 276–297. [CrossRef]
11. Gebremariam, S.N.; Marchetti, J.M. Biodiesel production technologies: Review. *AIMS Energy* **2017**, *5*, 425–457. [CrossRef]
12. Nguyen, H.C.; Liang, S.-H.; Doan, T.T.; Su, C.-H.; Yang, P.-C. Lipase-catalyzed synthesis of biodiesel from black soldier fly (Hermetica illucens): Optimization by using response surface methodology. *Energy Convers. Manag.* **2018**, *145*, 335–342. [CrossRef]
13. Singh, D.; Sharma, D.; Soni, S.L.; Sharma, S.; Sharma, P.K. A review on feedstocks, production processes, and yield for different generations of biodiesel. *Fuel* **2019**, *262*, 116553. [CrossRef]
14. Gnanaprakasam, A.; Sivakumar, V.M.; Surendhar, A.; Thirumarimurugan, M.; Kannadasan, T. Recent Strategy of Biodiesel Production from Waste Cooking Oil and Process Influencing Parameters: A Review. *J. Energy* **2013**, *2013*, 926392. [CrossRef]
15. Thangaraj, B.; Solomon, P.R.; Muniyandi, B.; Ranganathan, S.; Lin, L. Catalysis in biodiesel production—A review. *Clean Energy* **2019**, *3*, 2–23. [CrossRef]
16. Rizwanul Fattah, I.M.; Ong, H.C.; Mahlia, T.M.I.; Mofijur, M.; Silitonga, A.S.; Ashrafur Rahman, S.M.; Ahmad, A. State of the Art of Catalysts for Biodiesel Production. *Front. Energy Res.* **2020**, *8*, 101. [CrossRef]
17. Nasreen, S.; Nafees, M.; Qureshi, L.A.; Asad, M.S.; Sadiq, A.; Ali, S.D. Review of Catalytic Transesterification Methods for Biodiesel Production. In *Biofuels—State of Development*; IntechOpen: London, UK, 2018; pp. 94–111. [CrossRef]
18. Jin, H.; Kolar, P.; Peretti, S.W.; Osborne, J.A.; Cheng, J.J. Effect of preparation conditions on structure and activity of sodi-um-impregnated oyster shell catalysts for transesterification. *Catalysts* **2018**, *8*, 259. [CrossRef]
19. Alagumalai, A.; Mahian, O.; Hollmann, F.; Zhang, W. Science of the Total Environment Environmentally benign solid catalysts for sustainable biodiesel production: A critical review. *Sci. Total Environ.* **2021**, *768*, 144856. [CrossRef]
20. Shan, R.; Lu, L.; Shi, Y.; Yuan, H.; Shi, J. Catalysts from renewable resources for biodiesel production. *Energy Convers. Manag.* **2018**, *178*, 277–289. [CrossRef]
21. Goli, J.; Sahu, O. Development of heterogeneous alkali catalyst from waste chicken eggshell for biodiesel production Development of heterogeneous alkali catalyst from waste chicken eggshell for biodiesel production. *Renew. Energy* **2020**, *128*, 142–154. [CrossRef]
22. Vieira, S.S.; Magriotis, Z.M.; Ribeiro, M.F.; Graça, I.; Fernandes, A.; Lopes, J.M.F.M.; Coelho, S.M.; Santos, N.A.V.; Saczk, A.A. Use of HZSM-5 modified with citric acid as acid heterogeneous catalyst for biodiesel production via esterification of oleic acid. *Microporous Mesoporous Mater.* **2015**, *201*, 160–168. [CrossRef]
23. Sistani, A.; Saghatoleslami, N.; Nayebzadeh, H. Influence of calcination temperature on the activity of mesoporous CaO/TiO_2–ZrO_2 catalyst in the esterification reaction. *J. Nano Struct. Chem.* **2018**, *8*, 321–331. [CrossRef]
24. Meng, D.; Wang, B.; Yu, W.; Wang, W.; Li, Z.; Ma, X. Effect of Citric Acid on MoO_3/Al_2O_3 Catalysts for Sulfur-Resistant Methanation. *Catalysts* **2017**, *7*, 151. [CrossRef]
25. Li, J.; Liu, Y.; Gao, Y.; Zhong, L.; Zou, Q.; Lai, X. Preparation and properties of calcium citrate nanosheets for bone graft sub-stitute. *Bioengineered* **2016**, *7*, 376–381. [CrossRef]
26. Karthikeyan, B.; Govindhan, R.; Amutheesan, M. Chemical Methods for Synthesis of Hybrid Nanoparticles. In *Noble Metal-Metal Oxide Hybrid Nanoparticles: Fundamentals and Applications*; Elsevier Inc.: Amsterdam, The Netherlands, 2018. [CrossRef]
27. de Almeida, R.M.; Noda, L.K.; Gonçalves, N.S.; Meneghetti, S.M.P.; Meneghetti, M.R. Transesterification reaction of vegetable oils, using superacid sulfated TiO_2-base catalysts. *Appl. Catal. A Gen.* **2008**, *347*, 100–105. [CrossRef]
28. Venkatesha, N.J.; Ramesh, S. Citric Acid-Assisted Synthesis of Nanoparticle Copper Catalyst Supported on an Oxide System for the Reduction of Furfural to Furfuryl Alcohol in the Vapor Phase. *Ind. Eng. Chem. Res.* **2018**, *57*, 1506–1515. [CrossRef]
29. Labet, M.; Thielemans, W. Citric acid as a benign alternative to metal catalysts for the production of cellu-lose-grafted-polycaprolactone copolymers. *Polym. Chem.* **2012**, *3*, 679–684. [CrossRef]
30. Banković-Ilić, I.B.; Miladinović, M.R.; Stamenković, O.S.; Veljković, V.B. Application of nano CaO–based catalysts in biodiesel synthesis. *Renew. Sustain. Energy Rev.* **2017**, *72*, 746–760. [CrossRef]
31. Wen, L.; Wang, Y.; Lu, D.; Hu, S.; Han, H. Preparation of KF/CaO nanocatalyst and its application in biodiesel production from Chinese tallow seed oil. *Fuel* **2010**, *89*, 2267–2271. [CrossRef]
32. Helwani, Z.; Othman, M.R.; Aziz, N.; Kim, J.; Fernando, W.J.N. Solid heterogeneous catalysts for transesterification of tri-glycerides with methanol: A review. *Appl. Catal. A Gen.* **2009**, *363*, 1–10. [CrossRef]
33. Sihaib, Z.; Puleo, F.; Pantaleo, G.; Parola, V.; La Valverde, L.; Gil, S.; Liotta, L.F.; Giroir-fendler, A. The Effect of Citric Acid Concentration on the Properties of $LaMnO_3$ as a Catalyst for Hydrocarbon Oxidation. *Catalysts* **2019**, *9*, 226. [CrossRef]
34. Kaduk, J.A. Crystal structures of tricalcium citrates. *Powder Diffr.* **2018**, *33*, 98–107. [CrossRef]
35. Rammohan, A.; Kaduk, J.A. Trisodium citrate, $Na_3(C_6H_5O_7)$. *Acta Crystallogr. Sect. E Crystallogr. Commun.* **2016**, *72*, 793–796. [CrossRef] [PubMed]
36. Herdtweck, E.; Kornprobst, T.; Sieber, R.; Straver, L.; Plank, J. Crystal structure, synthesis, and properties of tri-Calcium di-citrate tetra-hydrate $[Ca_3(C_6H_5O_7)\ 2(H_2O)_2]\cdot 2H_2O$. *Z. Fur Anorg. Und Allg. Chem.* **2011**, *637*, 655–659. [CrossRef]

37. Wang, B.W.; Meng, D.J.; Wang, W.H.; Li, Z.H.; Ma, X.B. Effect of citric acid addition on MoO_3/CeO_2-Al_2O_3 catalyst for sulfur-resistant methanation. *J. Fuel Chem. Technol.* **2016**, *44*, 1479–1484. [CrossRef]
38. Radfarnia, H.R.; Iliuta, M.C. Limestone acidification using citric acid coupled with two-step calcination for improving the CO_2 sorbent activity. *Ind. Eng. Chem. Res.* **2013**, *52*, 7002–7013. [CrossRef]
39. Macina, A.; De Medeiros, T.V.; Naccache, R. A carbon dot-catalyzed transesterification reaction for the production of biodiesel. *J. Mater. Chem. A* **2019**, *7*, 23794–23802. [CrossRef]
40. Yao, J.; Gao, J.; Yao, J.; Zhu, B. Method for Preparing Anhydrous Trisodium Citrate. China Patent No. PCT/CN2016/108193, 2016. Available online: https://patentscope.wipo.int/search/en/detail.jsf?docId=WO2018094757&tab=FULLTEXT (accessed on 9 March 2021).
41. Zheng, L.; Li, Q.; Zhang, J.; Yu, Z. Double the biodiesel yield: Rearing black soldier fly larvae, Hermetia illucens, on solid residual fraction of restaurant waste after grease extraction for biodiesel production. *Renew. Energy* **2012**, *41*, 75–79. [CrossRef]
42. Bhargavi, G.; Nageswara Rao, P.; Renganathan, S. Review on the Extraction Methods of Crude oil from all Generation Biofuels in last few Decades. *IOP Conf. Ser. Mater. Sci. Eng.* **2018**, *330*, 012024. [CrossRef]
43. Kandaramath Hari, T.; Yaakob, Z. Effect of calcination temperature on the application of sodium zirconate solid base catalyst for biodiesel production from Jatropha curcas oil. *Int. J. Green Energy* **2017**, *14*, 1163–1171. [CrossRef]
44. Tanabe 2020, K.; Yamaguch, T. Basicity and Acidity of Solid Surfaces. *J. Res. Inst. Catal.* **1964**, *11*, 179–184.
45. Anr, R.; Saleh, A.A.; Islam, S.; Hamdan, S.; Maleque, A. Biodiesel Production from Crude Jatropha Oil using a Highly Active Heterogeneous Nanocatalyst by Optimizing Transesteri fi cation Reaction Parameters. *Energy Fuels* **2015**, *30*, 334–343. [CrossRef]
46. Asakuma, Y.; Maeda, K.; Kuramochi, H.; Fukui, K. Theoretical study of the transesterification of triglycerides to biodiesel fuel. *Fuel* **2009**, *88*, 786–791. [CrossRef]
47. Musa, I.A. The effects of alcohol to oil molar ratios and the type of alcohol on biodiesel production using transesterification process. *Egypt. J. Pet.* **2016**, *25*, 21–31. [CrossRef]
48. Thanh, L.T.; Okitsu, K.; Boi, L.; Van Maeda, Y. Catalytic Technologies for Biodiesel Fuel Production and Utilization of Glycerol: A Review. *Catalysts* **2012**, *2*, 191–222. [CrossRef]
49. Chisti, Y. Biodiesel from microalgae. *Biotechnol. Adv.* **2007**, *25*, 294–306. [CrossRef]
50. Trejo-Zárraga, F.; de Jesús Hernández-Loyo, F.; Juan, C.C.-H.; Sotelo-Boyás, R. Kinetics of Transesterification Processes for Bio-diesel Production. In *Biofuels—State of Development*; IntechOpen: London, UK, 2018; p. 13. [CrossRef]
51. Lawan, I.; Garba, Z.N.; Zhou, W.; Zhang, M.; Yuan, Z. Synergies between the microwave reactor and CaO/zeolite catalyst in waste lard biodiesel production. *Renew. Energy* **2020**, *145*, 2550–2560. [CrossRef]
52. *ASTM D6751-09*; Standard Specification for Biodiesel Fuel Blend Stock (B100) For Middle Distillate Fuels. ASTM International: West Conshohocken, PA, USA, 2009. [CrossRef]
53. Jiang, X.C.; Chen, C.Y.; Chen, W.M.; Yu, A.B. Role of citric acid in the formation of silver nanoplates through a synergistic reduction approach. *Langmuir* **2010**, *26*, 4400–4408. [CrossRef]
54. Tao, G.; Hua, Z.; Gao, Z.; Zhu, Y.; Zhu, Y.; Chen, Y.; Shu, Z.; Zhang, L.; Shi, J. KF-loaded mesoporous Mg–Fe bi-metal oxides: High performance transesterification catalysts for biodiesel production. *Chem. Commun.* **2013**, *49*, 8006–8008. [CrossRef]
55. Mierczynski, P.; Szkudlarek, L.; Chalupka, K.; Maniukiewicz, W.; Wahono, S.K.; Vasilev, K.; Szynkowska-jozwik, M.I. The Effect of the Activation Process and Metal Oxide Addition (CaO, MgO, SrO) on the Catalytic and Physicochemical Properties of Natural Zeolite in Transesterification Reaction. *Materials* **2021**, *14*, 2415. [CrossRef]
56. Tang 1963, Y.; Xu, J.; Zhang, J.; Lu, Y. Biodiesel production from vegetable oil by using modified CaO as solid basic catalysts. *J. Clean. Prod.* **2013**, *42*, 198–203. [CrossRef]
57. Yao, M.; Yao, N.; Liu, B.; Li, S.; Xu, L.; Li, X. Effect of SiO_2/Al_2O_3 ratio on the activities of CoRu/ZSM-5 Fischer-Tropsch synthesis catalysts. *Catal. Sci. Technol.* **2015**, *5*, 2821–2828. [CrossRef]
58. Wong, Y.C.; Tan, Y.P.; Taufiq-Yap, Y.H.; Ramli, I. Effect of calcination temperatures of CaO/Nb_2O_5 Mixed Oxides Catalysts on Biodiesel Production. *Sains Malays.* **2014**, *43*, 783–790.
59. Tsai, W.T.; Yang, J.M.; Lai, C.W.; Cheng, Y.H.; Lin, C.C.; Yeh, C.W. Characterization and adsorption properties of eggshells and eggshell membrane. *Bioresour. Technol.* **2006**, *97*, 488–493. [CrossRef] [PubMed]
60. Akmaliyah, M. Highly Active CaO for the Transesterification to Biodiesel Production from Rapeseed Oil. *J. Chem. Inf. Model.* **2013**, *53*, 1689–1699.
61. Ahmad, R.; Rohim, R.; Ibrahim, N. Properties of Waste Eggshell as Calcium Oxide Catalyst. Appl. *Mech. Mater.* **2015**, *754–755*, 171–175. [CrossRef]
62. Giri, A.; Makhal, A.; Ghosh, B.; Raychaudhuri, A.K.; Pal, S.K. Functionalization of manganite nanoparticles and their inter-action with biologically relevant small ligands: Picosecond time-resolved FRET studies. *Nanoscale* **2010**, *2*, 2704–2709. [CrossRef]
63. Wang, L.; Li, J.; Jiang, Q.; Zhao, L. Water-soluble Fe_3O_4 nanoparticles with high solubility for removal of heavy-metal ions from waste water. *Dalton Trans.* **2012**, *41*, 4544–4551. [CrossRef]
64. Ding, Z.; Xu, W.; Zhang, X.; Liu, Z.; Shen, J.; Liang, J.; Jiang, M.; Ren, X. Controllable Acid/Base Propriety of Sulfate Modified Mixed Metal Oxide Derived from Hydrotalcite for Synthesis of Propylene Carbonate. *Catalysts* **2019**, *9*, 470. [CrossRef]
65. Arboleda, A.; Franco, M.; Caicedo, J.; Tirado, L.; Goyes, C. Synthesis and chemical and structural characterization of hydroxyapatite obtained from eggshell and tricalcium phosphate. *Ing. Y Compet.* **2016**, *18*, 69. [CrossRef]

66. Roy, A.; Bhattacharya, J. Microwave-assisted synthesis and characterization of CaO nanoparticles. *Int. J. Nanosci.* **2011**, *10*, 413–418. [CrossRef]
67. Arzamendi, G.; Campo, I.; Arguiñarena, E.; Sánchez, M.; Montes, M.; Gandía, L.M. Synthesis of biodiesel with heterogeneous NaOH/alumina catalysts: Comparison with homogeneous NaOH. *Chem. Eng. J.* **2007**, *134*, 123–130. [CrossRef]
68. Salem, M.A.; Bakr, E.A.; El-Attar, H.G. Pt@Ag and Pd@Ag core/shell nanoparticles for catalytic degradation of Congo red in aqueous solution. Spectrochim. Acta Part A Mol. *Biomol. Spectrosc.* **2018**, *188*, 155–163. [CrossRef] [PubMed]
69. Li, Q.; Zheng, L.; Cai, H.; Garza, E.; Yu, Z.; Zhou, S. From organic waste to biodiesel: Black soldier fly, Hermetia illucens, makes it feasible. *Fuel* **2011**, *90*, 1545–1548. [CrossRef]
70. Pang, W.; Hou, D.; Ke, J.; Chen, J.; Holtzapple, M.T.; Tomberlin, J.K.; Chen, H.; Zhang, J.; Li, Q. Production of biodiesel from CO_2 and organic wastes by fermentation and black soldier fly. Renew. *Energy* **2020**, *149*, 1174–1181. [CrossRef]
71. Qing, L.; Zheng, L.; Qiu, N.; Cai, H.; Tomberlin, J.K.; Yu, Z. Bioconversion of dairy manure by black soldier fly (Diptera:Stratiomyidae) for biodiesel and sugar production. *Waste Manag.* **2011**, *31*, 1316–1320. [CrossRef]
72. Serrano, M.; Bouaid, A.; Martínez, M.; Aracil, J. Oxidation stability of biodiesel from different feedstocks: Influence of com-mercial additives and purification step. *Fuel* **2013**, *113*, 50–58. [CrossRef]
73. Peer, M.S.; Kasimani, R.; Rajamohan, S.; Ramakrishnan, P. Experimental evaluation on oxidation stability of biodiesel/diesel blends with alcohol addition by rancimat instrument and FTIR spectroscopy. *J. Mech. Sci. Technol.* **2017**, *31*, 455–463. [CrossRef]
74. Joven, J.M.O.; Gadian, J.T.; Perez, M.A.; Caingles, J.G.; Mansalaynon, A.P.; Ido, A.L.; Arazo, R.O. Optimized ultrasonic-assisted oil extraction and biodiesel production from the seeds of Maesopsis eminii. *Ind. Crops Prod.* **2020**, *155*, 112772. [CrossRef]
75. Lawan, I.; Zhou, W.; Idris, A.L.; Jiang, Y.; Zhang, M.; Wang, L.; Yuan, Z. Synthesis, properties and effects of a multi-functional biodiesel fuel additive. *Fuel Process. Technol.* **2020**, *198*, 106228. [CrossRef]
76. Leong, S.Y.; Kutty, S.R.M.; Malakahmad, A.; Tan, C.K. Feasibility study of biodiesel production using lipids of Hermetia illucens larva fed with organic waste. *Waste Manag.* **2016**, *47*, 84–90. [CrossRef]
77. De Sousa, F.P.; Dos Reis, G.P.; Cardoso, C.C.; Mussel, W.N.; Pasa, V.M.D. Performance of CaO from different sources as a catalyst precursor in soybean oil transesterification: Kinetics and leaching evaluation. *J. Environ. Chem. Eng.* **2016**, *4*. [CrossRef]
78. Pandit, P.R.; Fulekar, M.H. Egg shell waste as heterogeneous nanocatalyst for biodiesel production: Optimized by response surface methodology. J. *Environ. Manag.* **2017**, *198*, 319–329. [CrossRef] [PubMed]